J Ther Eng, Vol. 9, No. 6, pp. 1548−1558, November, 2023

Journal of Thermal Engineering
Web page info: https://jten.yildiz.edu.tr
DOI: 10.18186/thermal.1401040

Journal of Thermal Engineering

Research Article

Drying model based on the relative humidity profile of thin-layer tomatoes in an indirect solar dryer

Ahmed ALAMI[1], Lala RAJAOARISOA[2], Mohammed-Hichem BENZAAMA[3], Abdeldjalil BENBAKHTI[4]

[1]*Department of Automatic, University Djilali Liabes, Faculty of Electrical Engineering, Lab of Process Engineering Materials and Environment, Sidi Bel Abbes, 22000, Algérie*
[2]*IMT Nord Europe, Université de Lille, CERI Syst. Num´eriques, F-59500, Douai, 59000, France*
[3]*NU COMUE Normandie Universite - Laboratoire de Recherche ESITC - ESITC Caen. Rue Pierre et Marie Curie 14610 Epron, 14032, France*
[4]*Department of Hydraulics, University Centre of Maghnia, N99 Road of Zouia, Maghnia, Tlemcen, 13001, Algeria*

ARTICLE INFO

Article history
Received: 30 January 2023
Revised: 14 April 2023
Accepted: 18 April 2023

Keywords:
Drying Model; Experimental Model; Drying Dynamics; Dryer Design

ABSTRACT

This work defined the development of a model for thin-film drying of tomatoes using an indirect solar dryer. Drying experiments were carried out and the drying model was approximated by a simplified model determined by the measurements collected during the experiments, in particular, the measurement of the relative humidity of the tomato during two days of drying coupled with the thermal behaviour of the drying device in free convection. The results show that with good measurements, it is possible to approximate the drying characteristic curve by a linear model with very high statistical performance indicators. The experiments also show that depending on the drying process adopted, the water behaviour of the tomato can change. In addition, the thin-film drying model adopted made it possible to assess the solar drying kinetics of the tomato variety studied. The results obtained finally show that the dryness of the tomato is reached after about 14 hours of drying. The drying temperature reaches an average of 80°C, and the final product water content after the optimal drying time is about 0.40 kg.water/kg.ms on a dry basis.
At the end of this study, we concluded that the drying air temperature represents the most important parameter affecting the drying kinetics. The very good agreement between the experimental and numerical results obtained shows that the theoretical model and assumptions used are acceptable, and that our calculation model is reliable.

Cite this article as: Alami A, Rajaoarisoa L, Benzaama MH, Benbakhti A. Drying model based on the relative humidity profile of thin-layer tomatoes in an indirect solar dryer. J Ther Eng 2023;9(6):1548−1558.

***Corresponding author.**
*E-mail address: alami.ahmed21@gmail.com

This paper was recommended for publication in revised form by Regional Editor Ahmet Selim Dalkılıç

INTRODUCTION

The use of solar energy has been the subject of many research works [1-2]. Nowadays, food is mainly dried using either an indirect solar dryer or a forced convection blower [3]. In any case, the purpose of drying products is to reduce the moisture content and to store them. This slows down the decomposition of the food due to the growth and multiplication of inhibited micro-organisms by removing moisture [4], which minimizes most of the damage caused by it. Dryness also helps to slow down enzyme activity, but does not completely block them because drying causes water loss, which makes food lighter in weight. When the food is ready to use, rehydration (adding water) can be done to return the food to its original state. Drying consumes a lot of heat, which reduces the moisture in the product, making it safe energy in the form of conduction, transformation, or radiation. Solar heating/drying processes food in a safe, clean, and hygienic manner and produces nutritious food. Solar dryers help save energy, time, space/area, and labor for the farmer to dry the product, making the process efficient while protecting the environment [5].

Sun drying is the most economical method; however, it has problems with food contamination from dust, rodents, insects, rot, rain, etc. In contrast, solar drying is an interesting alternative for the food industry as it reduces dependence on fossil fuels, protects food from environmental impacts, conditions, and exposure to sunlight, improving drying efficiency and product quality, which is better in terms of nutrition and color [6]. Food drying thus plays a very important role in agriculture and industry. However, the process is not easy to implement and control due to the complexity of the transfer mechanisms and the diversity of the products, as well as the lack of basic knowledge about the products themselves. In addition, in developed countries, there are many methods of preserving agricultural products, such as freezing, genetic manipulation of products, and many more. The problem is that genetic manipulation, for example, is costly and technically demanding, and freezing consumes a lot of energy because it is constantly being powered, which affects the cost of the product. Drying remains the most popular, effective, and economical method of preserving agricultural foods [7-8]. In order to reduce post-harvest losses and to facilitate the understanding of the process, the use of solar drying of agricultural products would be an advantageous solution. Drying in the open air is the easiest method, from paleo to dry produce, ready-to-dry produce sprayed in the sun, light up on plastic, metal panels or directly on the ground. The sun is an uncontrolled energy source whose strength depends on various weather factors [9]. With direct solar dryers, the sun's rays are absorbed directly by products stored in cabinets. This drying cabinet is also known as a natural convection cabinet. Such solar dryers have compartments for storing covered products with clear glass or plastic or acrylic cover. The drying cabinet usually has an insulating flat sealed case that also allows air to flow from the atmosphere into the drybox [10]

To overcome the inconvenience caused by the growth and multiplication of microorganisms, and to ensure better control of the process, various research studies have been carried out for decades to develop the dehydration technique using solar dryers. Several studies have been attributed to improving the performance of solar dryers by developing the technology of component design collectors [11]. It was concluded that the drying time was approximately the same for all considered dryers, whether natural or forced.

There are numerous designs and configurations of solar dryers cited in the literature. Solar dryers can be divided based on how solar energy is used for grilling [12-13], according to the mode of operation, natural or forced convection [14-15]. Both have been classified into active solar drying and non-resistant systems, which were further related to direct or circular solar dryers[16], and mixed types[17]. According to their boundaries and shapes, they are divided into a type of press or greenhouse. Circular type dryers are divided into chimney stump, roof, shelf, and den, with or without thermal warehouse [18].

There are many technical reports related to the cooling and drying efficiency of solar dryers. In this context, previous studies mainly focused on hybrid and indirect solar dryers. Hybrid Mode Solar Dryers have no fans and no forced convection system, which is why it is also called a passive dryer. This dryer harvests energy from incoming sun rays, and solar panels pass through the drying chamber. In indirect sunlight Dryers, the sun's heat is first collected by solar panels, then it is sent to the drying room for drying [16].

However, it was pointed out that the indirect dryer had a higher drying rate in cloudy weather. It was also reported that the compartment type of dryer was the most suitable for small scale [19]. Moreover, by increasing the air flow rate by using a suitable solar chimney, for example, it can be observed that the drying rate inside the indirect solar dryer can be significantly modified [20], which can be up to 33%. In a more recent work, researchers have studied and analyzed a mixed solar dryer equipped with a fan and a photovoltaic panel. The main objective of this work was to extend the effective drying period of the device beyond sunset [21].

In the same way, other researchers have proposed instead to design an indirect solar dryer with a device to follow the path of the sun [22]. The sun tracker was shown to reduce the drying time of tomato slices in the range of 16.6% to 36.3%.

However, to better understand all these phenomena, researchers and operators need a well-calibrated model to interpret the water behavior of dried food. In this context, numerical models have been developed, for example, in [23] and in [24], to reproduce the water and thermal behavior of a thermo-convective flow in an indirect solar dryer.

In theory, it has been confirmed that this type of dryer provides less devastating heat than direct heating for drying tomatoes, for example. The development of these numerical models is still fastidious and complex because the parameters of these models may not be calibrated correctly due to the lack of knowledge on the product studied [25]. Another alternative has been proposed by Lankouande et al. in [26], considering that the numerical heat transfer model of the drying device can be approximated by analogy using an electrical system. This type of model has proved its worth in estimating thermal behavior in buildings, for example [27]. In fact, the electrical model is inspired by Daguenet's method in [28] based on the different heat transfers within the drying device. Thus, the model is based on the following four analogies:

- Flux density −→ Electric current intensity,
- Temperature −→ Electrical potential,
- Heat transfer coefficient −→ Conductivity,
- Heat capacity −→ Electrical capacity.

It must be said that this model is already simpler to develop than the numerical models proposed in the articles cited above. The only disadvantage we find in this model is that it is difficult to interpret given the different non-linear relationships between the exchanges and thermo-convective flow within the dryer itself.

A good understanding of the solar drying process goes hand in hand with a better understanding of the physical phenomena. However, this is not always easy to interpret because of the lack of knowledge of the physical phenomena. Thus, this paper proposes a plausible alternative through experimental trials to have a more explicit drying model that should help solar dryer designers to adapt their products to specific market needs. This said the originality of the paper lies essentially in the proposal of a data-driven methodology for modelling and analysing an indirect solar dryer to circumvent the complexity of the intrinsic physical phenomena of the system itself.

Thus, having a more explicit drying model and a good understanding of the solar drying process, through a better understanding of the physical phenomena process, through a better understanding of the physical phenomena, becomes essential for solar dryer necessary for solar dryer designers to adapt their product to the specific needs of the market. economic and environmental situation of the day.

Faced with this challenge, we propose to develop a model for thin layer tomato drying using an indirect solar dryer in an experimental way. In other words, to set up an experimental protocol and determine the drying model by using a simplified model obtained from the measurements collected during the experiments, in particular the measurement of the relative humidity of the tomato coupled with the thermal behaviour of the drying device. It should be noted that this type of approach has been tested for other products subject to drying and dehumidification cycles, as was studied in [29]. Therefore, in this paper we will show that the availability of measurements allows us to approximate the drying characteristic curve by a linear model with very high statistical performance indicators. And even though the model is linear, The feedback will also show that depending on the drying process adopted the hydric behaviour of the tomato can evolve.

Paper Organization

This paper will be organised in the following way. In Section 2, we will introduce the equivalent electrical model of the water behaviour of a thin tomato slice. We will also present the formulation of the data driven water model. On the other hand, Section 3 will present the methodology adopted to identify the parameters of the proposed model. Section 4 will discuss the results and provide explanations of the observed phenomena. Finally, the conclusions drawn from this experiment will be given in 5.

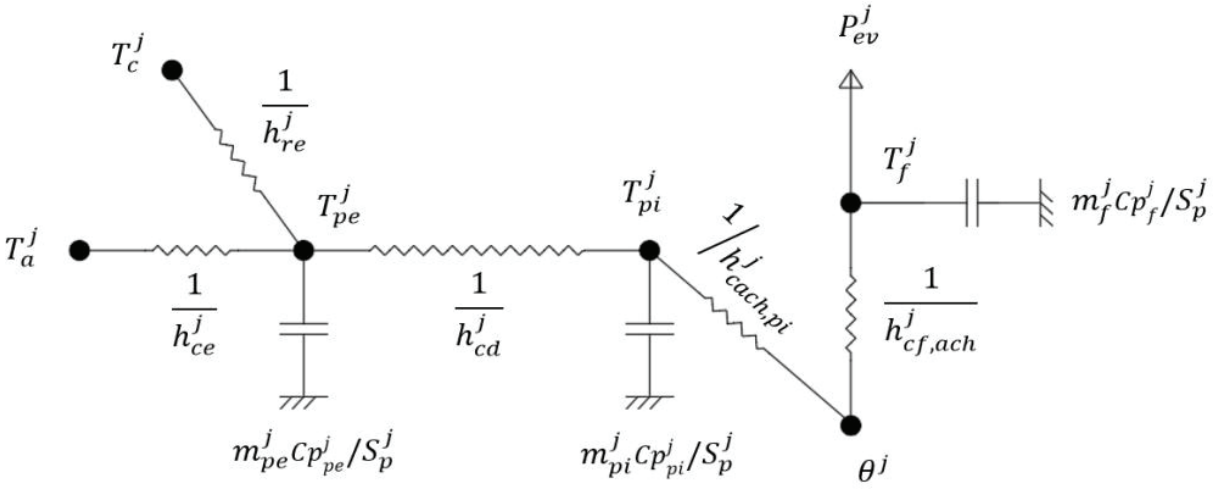

Figure 1. Equivalent electrical model of a drying device [26].

T_c^j represents the temperatures of the celestial vault, m_f^j the mass of the products by slice, m_{Fi}^j the mass of inner wall by slice, m_{pe}^j the external wall mass by slice, P_{ev}^j the evaporative power, $h_{Cf\cdot ach}^j$ ach the convective heat exchange coefficient between the air and the products, $h_{cach,pi}^j$ the convective heat exchange coefficient between the air and the internal wall, h_{Cd}^j the coefficient of heat exchange by conduction through the wall, h_e^j the convective heat exchange coefficient between the external wall and the outside air, h_{re}^j the radiation heat exchange coefficient between the external wall and the vault, Cp_{pe}^j the heat capacity of the wall.

METHODOLOGY

Hydric Drying Model

As mentioned earlier, physical equations can be used to express the hydric drying model. However, these equations are complex and difficult to handle, and it may be challenging to calibrate the parameters of the model due to limited knowledge about the product being studied. To address these issues, an alternative approach proposed in the literature is to use an approximate model based on an electrical analogy. This method will be discussed in the following paragraph.

Equivalent Electrical Model

Figure 1 above is based on the analogy between the heat transfer and the equivalent electrical transfer of a solar drying device, consisting essentially of nodes where the thermal dynamics can be observed. The heat and mass balance equations at the different nodes of the materials of which the dryer is made, leads to the following expressions.

Assuming the different temperatures of the nodes as [15] ($T_{pe}{}^j, T_{pi}{}^j, T_f^j, \theta^j$), the energy balance on each node for a slice (j) of the dryer is written : At the external wall :

$$m_{pe}^j C_{pe}^j \frac{dT_P^j}{dt} = h_{Cc} S_p^j \left(T_a^j - T_{P=}^j\right) + h_j^{re} S_p^j + \left(T_j^{\varepsilon} - T_{pc}^j\right) + h_{cf,ach}^j S_P^j + (T\} - \theta^{j-1}\Big) \quad (1)$$

On the internal wall :

$$m_{\mathrm{Fi}}^j C j_{P\mathrm{pi}} \frac{dT_{\mathrm{Fi}}^j}{dt} = h_{Cd}^j S j_p \left(T_{pc}^j - T_{pi}^j\right) + h_{cach,pi}^j S_F^j \left(\theta_p^{j-1} - T_{\mathrm{Fi}}^j\right) \quad (2)$$

In the air :

$$Q C_p \left(\theta_{\_} - \theta_{j-1}\right) = h h_{p-1} S_p \left(T_p - \theta_{j-1}\right) + h_{pch} S_p \left(T_p - \theta_{j-1}\right) \quad (3)$$

On the product level:

$$m_f^j C_{Pf}^j \frac{dT_f^j}{dt} = h_{Cf\cdot ach}^j S_p^j \left(\theta^{j-1} - T_F^j\right) \quad (4)$$

This equation governs the heat exchange of a slice (j) of the dryer placed in the ambient air. Assuming that the moisture profile of the tomato slices arranged in a thin layer is uniform and that their average water content during drying is given by the desorption isotherm under the conditions of the drying air, for a fictitious slice (j) of the dryer, the balances between the instants tj and $tj + \Delta t$, with (Δt) infinitely small, are obtained by writing the relative flux equilibria at the nodes of the network. We will linearise and discretise them. To carry out this work, we will use the di method after discretisation.

- At the external wall

$$m_{pe}^j C_{Ppe}^j \frac{T_{pe}^{(tj+\Delta t)} - T_{pc}^j}{\Delta t} = h_{Ce}^j S_p^j \left(T_a^j - T_{Pe}^{t_j+\Delta t}\right) + h_{re}^j S_P^j \left(T_c^j - T_{pe}^{tj+\Delta t}\right) + h_{ad}^j S_{pe}^j \left(T_{pe}^{tj+\Delta t} - T_{pe}^{tt_j+\Delta t}\right) \quad (5)$$

- On the internal wall :

$$m_{pi}^j C_{Pi}^j \frac{T_{pi}^{(tj+\Delta t)} - T_{pi}^j}{\Delta t} = h_{Cd}^j S_p^j \left(T_{pe}^j - T_{pi}^{t_j+\Delta t}\right) + h_{\mathrm{coach},pi}^j S_p^j \left(\theta^{(t_{j-1+\Delta t})} - T_{pi}^{tj+\Delta t}\right) \quad (6)$$

- In the air :

$$Q^j C_P^j \left(T^{(tj+\Delta t)} - \theta^{tj-1+\Delta t}\right) = h_{ach,pi}^j S_p^j \left(T_{pi}^{(tj+\Delta t)} - \theta^{t_j-1+\Delta t}\right) + + h_{cf,ach}^j S_p^j \left(T_f^{(t_j-1+\Delta t)} - \theta^{t_j-1+\Delta t^2}\right) \quad (7)$$

- On tomatoes level: :

$$m_f^j C f_f \frac{T_f^{(tj+\Delta t)} - T_{pf}^{tj}}{\Delta t} = h_{cf,ach}^j S_P^j \left(T_{pi}^{(tj+\Delta t)} - \theta^{tj-1+\Delta t}\right) + \left(\theta^{(t_j-1+\Delta t)} - T_f^{t_j+\Delta t}\right) - P_{cv}^j \quad (8)$$

From these equations, it is evident that even an equivalent numerical model based on an electrical analogy requires numerous parameters to be determined and controlled. To simplify the study of heat transfer in the solar air collector, the so-called global method of analysis is used, which assumes that the thermal inertia of the collector's components has a small time variation. Thus, the global method of analysis makes the simplifying assumption that the thermal inertia of the collector's components has a small time variation, allowing us to safely assume that the collector operates in a quasi-stationary state. The model also neglects heat losses by radiation and convection at the back of the collector. This confirms that a simplified mathematical model can be helpful in understanding the hygrothermal behavior of a dried product in a drying device.

Experimental Numerical Model

The proposed model to be used in this paper is a linear equation model fed by input-output data pairs. in this

context, the autoregressive equation with exogenous inputs (ARX) is one of the most widely used models to represent a dynamic system in a simple form. An ARX model aims to find a mathematical relationship between the output of the system and its past instances (the autoregressive part that represents the dynamic aspect of the system) and the inputs (the exogenous variables). The relationship in its simplest form for an output $y(t)$ and an input $u(t)$ is given as follows [19]:

$$y(t) + a_1 y(t-1) + \cdots + a_{na} y(t-n_a) = b_1 u(t-n_k) + \cdots + b_{nb} u(t-n_b-n_k+1) + e(t) \quad (9)$$

Where, $y(t)$ is the output measured at each time $t \in \mathbf{Z}$, $u(t)$ is the input measured at each time t and $e(t)$) defined as the effect of the measurement disturbances assumed to follow a normal distribution $N(0,\sigma^2)$. n_a, n_b the pure time delay between the inputs and the outputs. The coefficients b_i and a_i the model parameters to be determined.

To express the value of each new measured value we can rewrite (9) as follows:

$$y(t) = -a_1 y(t-1) + \cdots - a_{na} y(t-n_a) + b_1 u(t-n_k) + \cdots + b_{nb} u(t-n_b-n_k+1) + e(t) \quad (10)$$

Where the current output $y(t)$ is determined by its former values n_a and the n_b previous values of its inputs. The estimated value of this output can be described as follows:

$$\bar{y}(t) = -a_1 y(t-1) + \cdots - a_{na} y(t-n_a) + b_1 u(t-n_k) + \cdots + b_{nb} u(t-n_b-n_k+1) + e(t) \quad (11)$$

Thus, the parameters to be identified can be recombined in the following parameter vector:

$$\Lambda = [-a_1 \ldots - a_{na} b_{nk} \ldots b_{n_b+n_k-1}] \quad (12)$$

And the regression vector (for a multi-input, multi-output model) can be defined as:

$$\varphi(t) = [y(t-1) \ldots y(t-n_a) \ldots u(t-n_b) \ldots u(t-n_b-n_k+1)]^T. \quad (13)$$

Therefore, equation (10)) can be rewritten as follows:

$$y(t) = \Lambda^T \varphi(t) + e(t) \quad (14)$$

With f a random affine function having as its principal parameter the vector θ. In other words, for a pure linear function, the output of the model can be rewritten as follows:

$$y(t) = \Lambda^T \varphi(t) + e(t) \quad (15)$$

And equation (11) as:

$$\hat{y}(t) = \Lambda^T \varphi(t) \quad (16)$$

The solution of these equations, which is the value of the parameter vector Λ, is found by applying the least squares estimation which consists in minimising the cost function defined as the "*2-norm* " " of the difference between the estimated and measured output vectors, as a function of the unknown parameters Λ :

$$J(\Lambda) = \frac{1}{N}\sum_{t=1}^{N} (y(t) - \hat{y}(t))^2 = \frac{1}{N}\sum_{t=1}^{N} (y(t) - \Lambda^T \varphi(t))^2 \quad (17)$$

Where N cis the number of points collected on the system. The minimum is obtained here for this cost function when the gradient relative to the parameter Λ is close to zero. The solution to this optimisation problem is provided by the following normal equation:

$$\hat{\Lambda} = (\Phi^T \Phi)^{-1} \Phi^T Y \quad (18)$$

Where $Y = [y(1) \ldots y(N)]^T$ et $\Phi = [\varphi(1) \ldots \varphi(N)^T$.

Furthermore, to check that the current parameters, i.e. $\Lambda^{(r+1)}$, converge to an optimal value; we compare them with the previously obtained values, $\Lambda^{(r)} = \left[\hat{\Lambda}_1^{(r)}, \cdots, \hat{\Lambda}_s^{(r)}\right]$ with r as the number of iterations needed to converge the parameters. Thus, we can consider the following convergence criteria:

$$\|\Lambda^{(r+1)} - \Lambda^{(r)}\| \leq v \quad (19)$$

With v an arbitrary value of which will be defined by the user himself. Generally, we use $v = 10^{-5}$.

Finally, we consider two criteria to judge the relevance of the model parameters identified in this paper by the percentage value of the following standardised estimation error:

$$FIT = \left(1 - \frac{\|\hat{y} - y\|}{\|y - \bar{y}\|}\right) \times 100\%, \quad (20)$$

And the Root Mean Square Error used earlier to optimise the parameter calculation process :

$$MSE = \frac{1}{N}\sum_{t=1}^{N} (y(t) - \hat{y}(t))^2, \quad (21)$$

Where $\bar{y}$ and $\hat{y}$ are the average and the estimate of the $y(t)$measurements respectively.

RESULTS AND DISCUSSION

In order to proceed with the identification of the drying model, we adopt an ordered sequence of tests, each of

which allows us to gain new knowledge by controlling the input parameters in order to obtain results validating the drying model with the most reliable test possible. First of all, it should be recalled that the objective is to find the optimal parameters of the measurement- driven drying model that accurately reflects the physical relationships between the different elements of the device. To this end, after the design and configuration of the drying device, the next step in the methodology is to collect the measurements. In other words, we will have to instrument the device so that it reflects the different temperatures in the key areas of the device. Then we calculate the model parameters. In other words, we apply the steps listed in Section 2 above to identify the optimal values of the vector of parameters that minimise the J cost function. The identification of these parameters will then allow us to analyse the typical behaviours associated with the set of calculated parameters. The analysis will help us to improve the drying process and reconfigure the device to be more efficient. All these steps are illustrated in Figure 2.

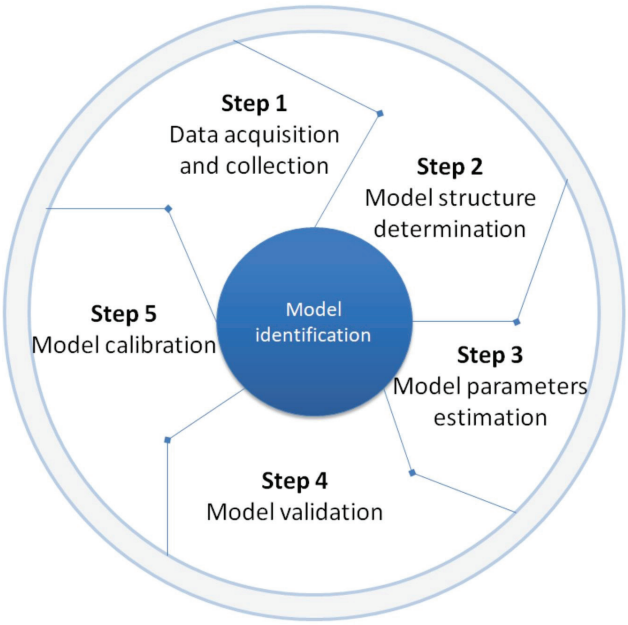

Figure 2. Different steps required to identify the model.

Description of the System

To model the drying behavior in the solar dryer, we propose calibrating the model based on experimentally available measurements of the relative humidity profile of the food. However, it is essential to optimize the orientation and inclination of the collector to capture the maximum amount of solar irradiation throughout the day. This requires considering the following factors:

- The inclination, which should be between 30° and 45° with respect to the horizon
- Its orientation, which should be predominantly south-facing
- Its azimuth, which should be adjusted to improve its mass of sunshine
- Its latitude, which should be taken into account to refine the solar irradiation time

The operation of the solar dryer is as follows: fresh air from the outside environment is first heated in the solar collector. The air absorber contact, as well as the convective and radiative heat transfer from the absorber to the air, are responsible for this heating process. The heated air then flows through the drying chamber where it removes moisture from the product being dried before being exhausted to the outside environment.

Heat transfer in the solar collector allows the air to be heated, raising its temperature. The heated air then enters the drying chamber and passes through the racks, further increasing the temperature and reducing the humidity through evaporation. To control the temperature and

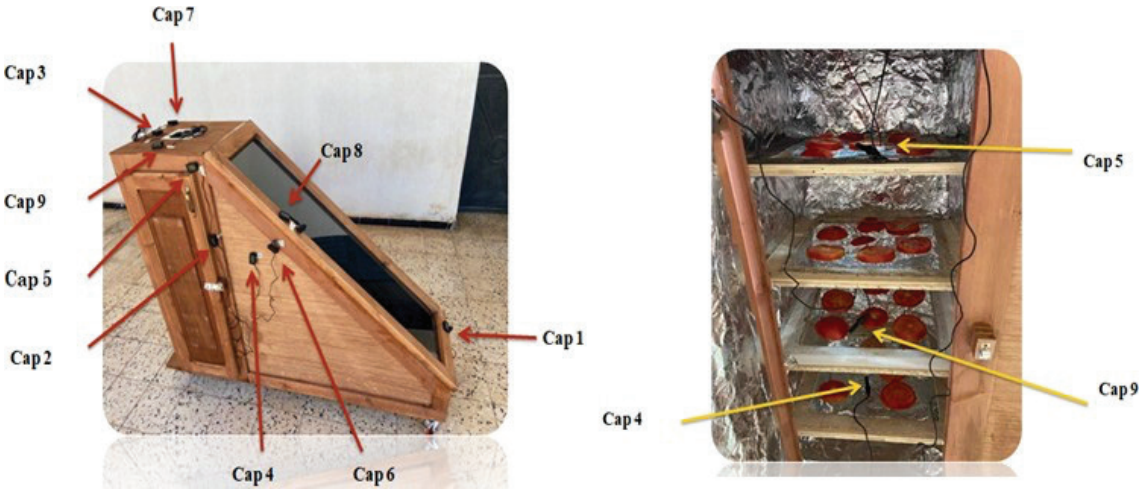

Figure 3. Illustration of the drying device and the tomato slices placed on its racks.

humidity, a digital thermostat W1209 is used as a switch to activate the extractor fan and expel the moist air outside. The investigated system, shown in Figure 3, is a well-insulated indirect solar dryer with dimensions of (120*110*50) cm. It consists of a transparent glass panel inclined at 45° (100*30)cm from the horizon, a drying chamber with four racks (45*45)cm, a black-coated absorbent plate at the base, and a fan (12V-10.1W-120mm) for moisture extraction.

The location is the city of Blida, Algeria, located at latitude 36.4808° N and longitude 2.8278° E. Using Blida's coordinates in Algeria and the date of June 15-16, 2022, we can obtain the following weather data:

- Maximum temperature: 38°C
- Minimum temperature: 18°C
- Solar radiation: 240 kWh/m²
- The relative humidity varies between 55% and 35%

Collecting Information

Experimental protocoll

The purchased tomato, washed and cut into 13mm thick slices, is spread out on the drying chamber racks (200g per rack). The weight loss of the product on the rack is monitored from the beginning of the experiment to the end, in other words from 10:00 to 17:00. The dryer is set at the temperature one hour before the start of the experiment to complete the transitional phase. The drying operation is considered complete when the equilibrium relative humidity of the product is reached, the value of the wet-base moisture content where the growth of any micro-organisms is inhibited. The temperature and relative humidity measurements are taken every 15 minutes, from which the moisture profile or drying kinetics of the product are traced as a function of time. At the end of each day the product is stored in airtight plastic boxes and placed in a refrigerator.

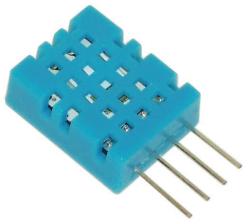

Figure 4. DHT-11 humidity and temperature sensor.

to avoid rehydration overnight and will keep its condition for the continuity of the operation in the following days. At the end of the drying operation, the dried samples are allowed to cool to ambient temperature and then sealed in plastic bags.

Measurement system

In our installation, we used a DHT-11 sensor whose characteristics are given in table 1 below. It consists of a capacitive humidity sensor and a high-precision temperature sensor with a wider measuring range, pr´esent in Figure 4. through an integrated 8-bit microcontroller. The DHT-11 converts the analogue output of these two sensors into a digital signal and transmits the temperature and humidity data via a single pin. [31]. The model was developed and programmed in the Matlab/Simulink environment. Then, in order to find the vector of parameters (defined by equation (12)) that minimises the cost function (equation (15)) we apply the least squares technique as defined in equation (16) in the paper.

In order to control the dryer and monitor the temperature and humidity values during the drying process, we have positioned the sensors in the following ways:

- Capteur 1 : Fresh air inlet
- Capteur 2: Absorber plate
- Capteur 3 Extractor (Fan)
- Capteur 4-5-9: Racks
- Capteur 6: Hot Air Inlet (below the racks)
- Capteur 7: External Environment
- Capteur 8: glazing

Figure 5 displays the changes in temperature over two days of experimental drying using a solar dryer. The graph shows temperature and humidity readings for different positions (1 to 9) of the sensors in the dryer, from 10:00 to 17:00 on each day. During the first day, the temperature increased gradually from 30°C to 50°C for most positions, with the exception of positions 1, 2, and 3, which had lower temperatures. The collectors 6 to 9, located at the glazing and absorbing plate, experienced the highest temperature increase due to the "greenhouse effect" and insulation of the dryer. The average temperature at these collectors reached 83°C, which is ideal for fast and efficient drying. On the second day, the temperature decreased after reaching its peak, especially at the center of the dryer, during sunset. It is important to note that the graph also shows humidity readings, which may also affect the drying process. Overall, the graph illustrates the effectiveness of the solar dryer in achieving high temperatures for rapid and efficient drying.

Table 1. Technical specifications of the DHT-11 sensor

Element	Measurement range	Accuracy in humidity	Temperature accuracy	Resolution	Disposition
DHT-11	20 – 90%*HR* 0 – 50°*C*	±5%*HR*	±2°*C*	1	4 Pin

Discussion and Validation of the Model

The lower part of Figure 6 below shows us the efficiency of the experimental numerical model based on the relative humidity profile of a thin layer of tomato in an indirect solar dryer. In this figure, the blue curve represents the measurement of the relative humidity at the of relative humidity at the tomato level and the one in red illustrates the estimation of this relative humidity rate by the developed hydric model. To evaluate the performance of the model presented, we only interpret the ITD and MSE values In this paper, we (see equations 20 and 21). To obtain such a result, the hyperparameters of the model were empirically evolved by taking into account values between 1 a` 5 for the parameters n_a, n_b and n_k. We found that the optimal values of FIT = 94.63% and MSE = 0.07244 are reached when we have the initialization parameters $n_a = 2$, $n_b = 2$ and $n_k = 0$.

Thus, we can say that the proposed model is remarkably successful in predicting the relative humidity of the tomato. We also notice that the drying of thin layer tomatoes is faster and reaches an ideal humidity and a perfect texture for a dehydrated and finalised product, without affecting the chemical and microbiological composition of the product. Indeed, we observe that the evolution of humidities for the nine sensors are regressive during the day from 80% (1^{er} day of drying) to 15% on the 2^{eme} day in relation to time, and ascending during sunset. In this configuration, we can calculate the final moisture content which is0, 4[*kg.eau/kg.ms*] of dry matter reached after 2 days of dehydration process

Furthermore, as explained above, at the end of each day we store the products in airtight plastic boxes and place them in a refrigerator to avoid rehydration during the night and so that they can keep their current state during the drying operation the next day. the following day. Thus, the dry samples were allowed to cool to ambient temperature and then sealed in plastic bags. After analysing the hydrous behaviour of the products, see the upper part of figure 6, we can see that this storage process indeed changes the typical behaviour of the product as two (2) typical drying behaviours are identified during the data analysis. The first one is the classical drying associated with the first day and

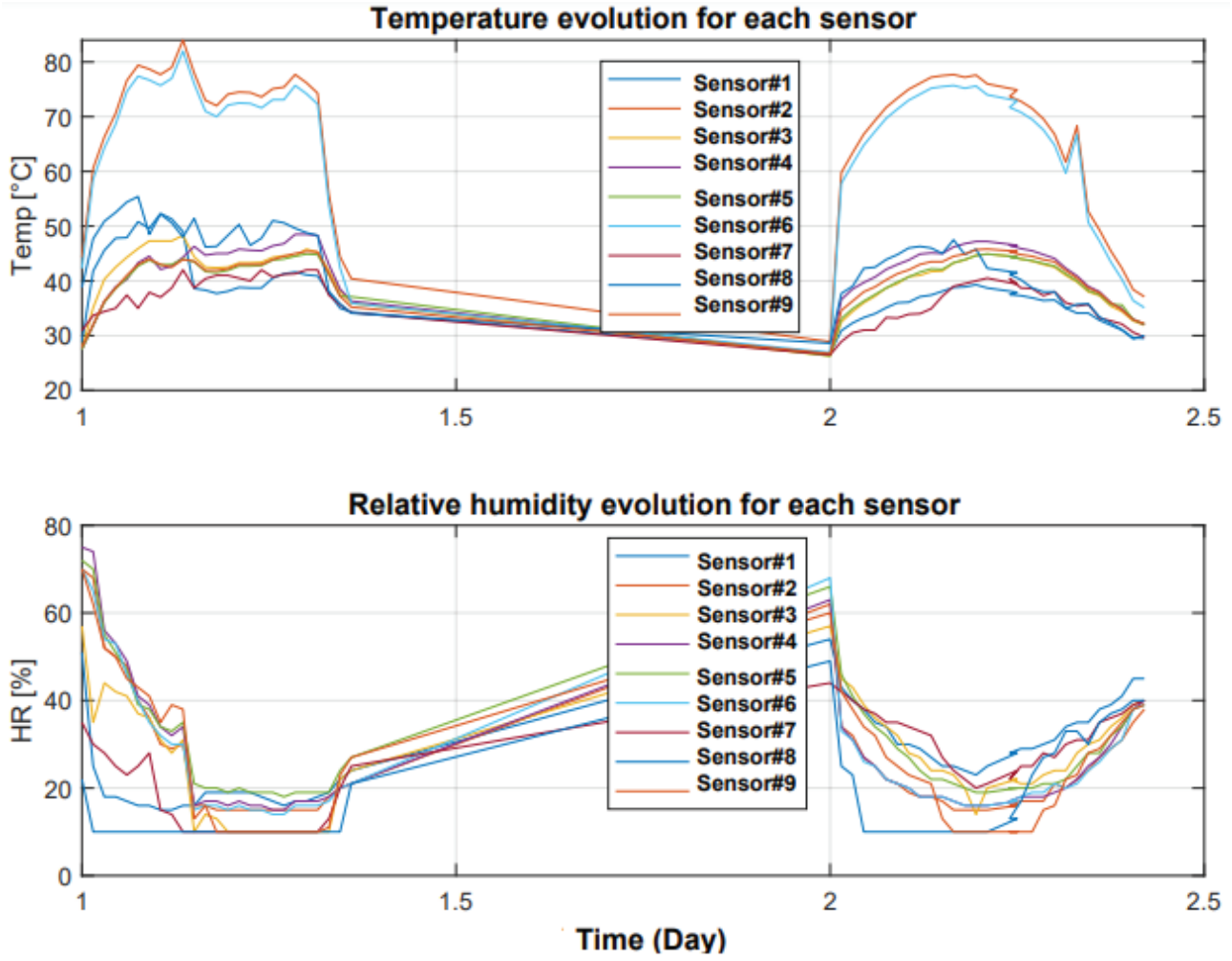

Figure 5. Temperature and relative humidity measurements at each sensor.

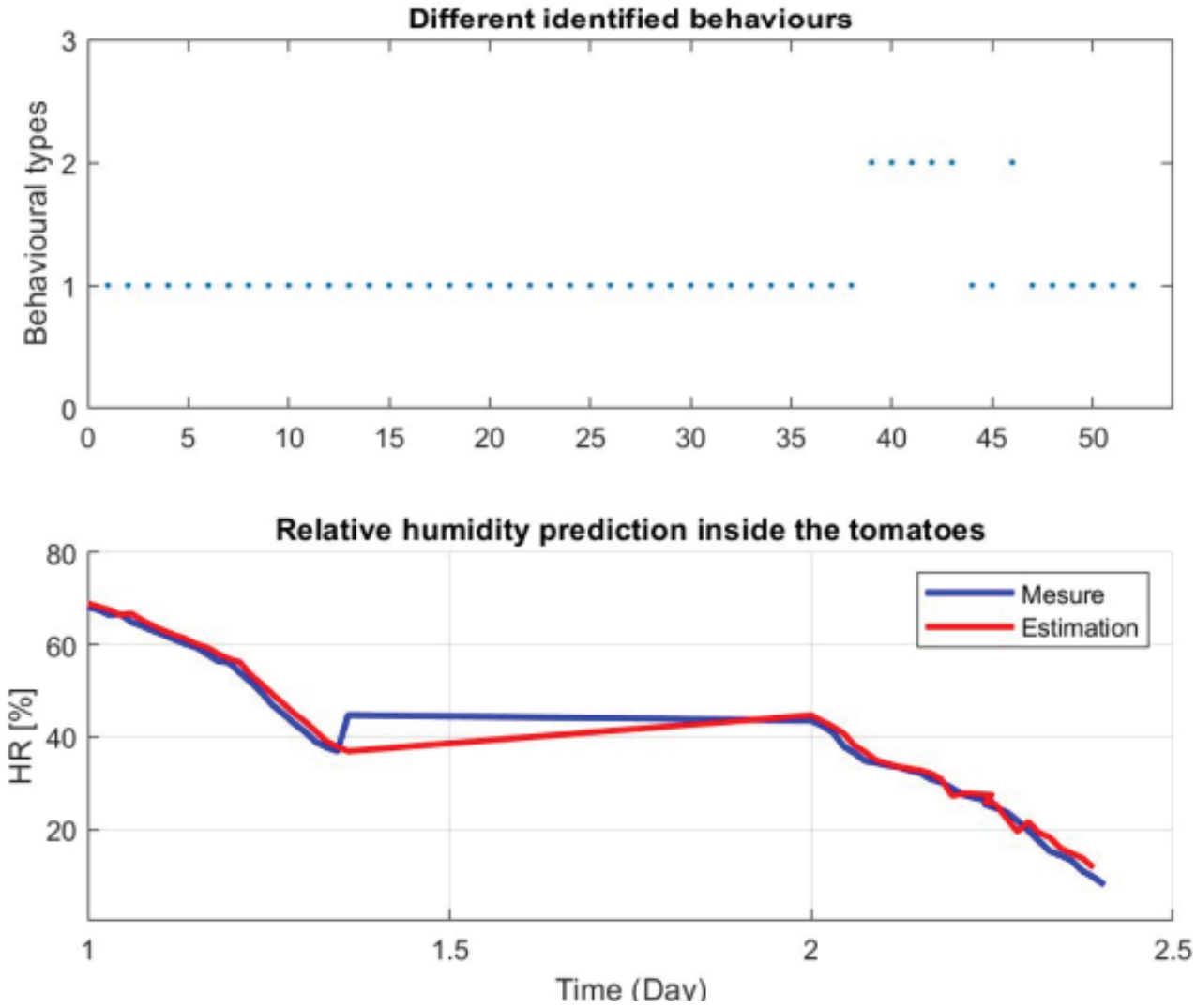

Figure 6. Validation of the experimental drying model.

Table 2. Table of initial and identified parameters

Parameters	Value	Correspondence			
n_a	2	Model order			
n_b	2	Model order			
n_k	0	Model order			
a	[0.9643 0]'	parameter connecting the model to	the	output	
b_1	[0.1642 -0.2578 -0.3612 -0.3439]'	parameter connecting the model with	the	sensor	1
b_2	[2.1811 0.3519 -0.2281 -0.4881]'	parameter connecting the model with	the	sensor	2
b_3	[-0.7402 -0.5769 -0.0789 0.1318]'	parameter connecting the model with	the	sensor	3
b_4	[0.2212 -0.311 0.1735 0.0733]'	parameter connecting the model with	the	sensor	4
b_5	[-0.7828 0.3868 -0.1065 0.099]'	parameter connecting the model with	the	sensor	5
b_6	[-2.0439 -0.2614 -0.1317 0.4152]'	parameter connecting the model with	the	sensor	6
b_7	[0.1383 0.4712 0.0865 0.0915]'	parameter connecting the model with	the	sensor	7
b_8	[-0.2358 -0.091 0.1271 -0.0827]'	parameter connecting the model with	the	sensor	8
b_9	[0.3580 0.2732 0.2598 0.0322]'	parameter connecting the model with	the	sensor	9

the second one is the start of the process on the second day. This raises the question of how we should store the food during the two drying phases or leads us to reflect on either the effective drying period of the appliance beyond sunset, or on improving the design of the drying device to make it more efficient and fast for a drying time of the order of one day. Finally, by analysing the parameters obtained in Table 2, we note that the measurements taken on sensors 2 and 6 have the most influence on the evolution of the water dynamics of the system. On reflection, this seems normal to us because these sensors record the temperature and the humidity level at the level of the absorbing plates and at the level of the hot air entry placed under the trays. We can deduce that if we want to improve our system, we should pay particular attention to these parameters by, for example, optimally controlling the temperature and humidity at the absorber plate and the incoming hot air by automated devices. We strongly hope that this analysis and experience could help solar dryer designers in their thinking to optimise their process as well.

CONCLUSION

The originality of our approach consists in a systematic recourse to experimentation for the development of a model of the thin layer tomato drying process using an indirect solar dryer. As it is difficult to control the drying operation in the natural convection dryer (flow velocity and temperature of the drying air in the dryer changing along the day depending on the atmospheric conditions), we propose in this paper a simplified model determined by the measurements collected during the experiments, in particular the measurement of the relative humidity of the tomato during two days of drying coupled with the thermal behaviour of the drying device. The study of the dryer with thin slices of tomato placed on racks allowed us to obtain a set of drying curves in order to detect the aerothermal parameters(humidity and temperature) of the drying air that have the greatest influence on the product drying process. The results also show that with good measurements, it is possible to approximate the drying characteristic curve by a linear model with very high statistical performance indicators. The experiments determined that depending on the drying process adopted, the water behaviour of the tomato can change. In addition, the thin layer drying model adopted allowed to appreciate the solar drying kinetics of the studied tomato variety. The results finally show that the dryness of the tomato is reached after about 14 hours of drying. The drying temperature reaches an average of 80°C, and the final product water content after the optimal drying time is about 0.40 kg.water/kg.ms in dry basis.

NOMENCLATURE

T	Temperature, °C
C_{p_f}	Specific heat, kJ / kg °C
h	Convective heat transfer coefficient, W/m. °C
P	Power evaporation, W
m	The mass of product, kg
$n_a, n_b \ldots$	Experimental model orders
$a_1, b_1, a_2, b_2 \ldots$	Model parameters
t	Discrete time s
$e(t)$	White noise
N	Number of collected samples

Greek symbols

υ	Arbitrary threshold value
$\hat{y}(t)$	Estimated output
$y(t)$	Measured output
Φ	Set of the regression vector
Λ	Vector of parameters
φ	Regression vector
$u(t)$	Model input

Abreviations

MSE	Mean Square Error
FIT	Fitting Error
N	Number of collected samples

AUTHORSHIP CONTRIBUTIONS

Authors equally contributed to this work.

DATA AVAILABILITY STATEMENT

The authors confirm that the data that supports the findings of this study are available within the article. Raw data that support the finding of this study are available from the corresponding author, upon reasonable request.

CONFLICT OF INTEREST

The author declared no potential conflicts of interest with respect to the research, authorship, and/or publication of this article.

ETHICS

There are no ethical issues with the publication of this manuscript.

REFERENCES

[1] Alami A, Boucham B, Gouareh A. Investigation on the energy efficiency of a geo-sol adsorption heat transformer in the Algerian context. Int J Heat Technol. 2019;37(3):820−830. [CrossRef]

[2] Alami A, Makhlouf M, Lousdad A, Khalfi A, Benzaama MH. Energetic and exergetic analyses of adsorption heat transformer ameliorated by ejector. J Braz Soc Mech Sci Eng. 2016;38:2077−2084. [CrossRef]

[3] Khama R, Aissani F, Alkama R. D'etermination expérimentale de la cinétique de séchage solaire de la tomate. In: Proceedings of the Deuxième Conférence Internationale sur les Energies Renouvelables et leurs Applications (ICRE'2012); 2012; Béjaïa, Algérie.
[4] Kamil S. Effect of drying methods on thin-layer drying characteristics of hullless seed pumpkin (Cucurbita pepo L.). J Food Eng. 2007;79(1):23−30. [CrossRef]
[5] Udomkun P, Romuli S, Schock S, Mahayothee B, Sartas M, Wossen T, et al. Review of solar dryers for agricultural products in Asia and Africa: An innovation landscape approach. J Environ Manage. 2020;268:110730. [CrossRef]
[6] Mehta P, Samaddar S, Patel P, Markam B, Maiti S. Design and performance analysis of a mixed mode tent-type solar dryer for fish-drying in coastal areas. Sol Energy. 2018;170:671−681. [CrossRef]
[7] Kumar M, Kumar S, Khatak PS. Progress in solar dryers for drying various commodities. Renew Sustain Energy Rev. 2016;55:346−360. [CrossRef]
[8] Nadeau J, Puiggali J. S'echage: des processus physiques aux proc'edes industriels. Energy Clean Environ. 1995;16(1-4):235−245.
[9] Mühlbauer W. Present status of solar crop drying. J Energy Agric. 1986;5(2):121−137. [CrossRef]
[10] Sharma A, Chen CR, Vu Lan N. Solar-energy drying systems: A review. Renew Sustain Energy Rev. 2009;13(6-7):1185−1210. [CrossRef]
[11] Slimani M, Amirat M, Bahria S. Study and modeling of heat transfer and energy performance in a hybrid pv/t collector with double passage of air. Int J Energy Clean Environ. 2015;16(1-4):235−245. [CrossRef]
[12] Chauhan YB, Rathod PP. A comprehensive review of the solar dryer. Int J Ambient Energy. 2020;41(3):348−367. [CrossRef]
[13] Ekechukwu OV, Norton B. Review of solar-energy drying systems II: an overview of solar drying technology. Energy Convers Manag. 1999;40(6):615−655. [CrossRef]
[14] Chaudhari AD, Salve SP. A review of solar dryer technologies. Int J Res Advent Technol. 2014;2(2): 218−232.
[15] Mustayen AGBM, Mekhilef S, Saidur R. Performance study of different solar dryers: a review. Renew Sustain Energy Rev. 2014;34:463−470. [CrossRef]
[16] Fudholi A, Sopian K, Ruslan MH, Alghoul MA, Sulaiman MY. Review of solar dryers for agricultural and marine products. Renew Sustain Energy Rev. 2010;14(1):1−30. [CrossRef]
[17] Sharma V, Colangelo A, Spagna G. Experimental investigation of different solar dryers suitable for fruit and vegetable drying. Renewable Energy. 1995;6(4):413−424. [CrossRef]
[18] Afriyie J, Nazha M, Rajakaruna H, Forson F. Experimental investigations of a chimney-dependent solar crop dryer. Renewable Energy. 2009;34(1):217−222. [CrossRef]
[19] Baniasadi E, Ranjbar S, Boostanipour O. Experimental investigation of the performance of a mixed-mode solar dryer with thermal energy storage. Renewable Energy. 2017;112:143−150. [CrossRef]
[20] Samimi-Akhijahani H, Arabhosseini A. Accelerating drying process of tomato slices in a pv-assisted solar dryer using a sun tracking system. Renewable Energy. 2018;123:428−438. [CrossRef]
[21] Kuan M, Ye S, Mohanraj M, Ye B, Jayaraj S, Kaltayev A. Numerical simulation of a heat pump assisted solar dryer for continental climates. Renewable Energy. 2019;143:214−225. [CrossRef]
[22] Arun K, Kunal G, Srinivas M, Kumar C, Mohanraj M, Jayaraj S. Drying of untreated musa nendra and momordica charantia in a forced convection solar cabinet dryer with thermal storage. Energy. 2020;192:116697. [CrossRef]
[23] Mariem S, Mabrouk S. Cinétique de séchage et courbe caractéristique de séchage d'une couche mince de tomate. In: Proceedings of the International Congres on Thermal Processes / Journée Internationale de Thermique- JITH2017; October 2017; Monastir, Tunisie.
[24] Lankouande R, Frédéric O, Palm K, Kam S. Modélisation et expérimentation du séchage solaire indirect en couches minces de tranches de tomates de la variété mongal. Eur J Sci Res. 2020;156(1):22−32.
[25] Randriatsiferana R, Rajaoarisoa L, Ngoho S, Rahajandraibe W, Ravelo B. Zonal thermal room original model with kron's method. IEEE Access Trans. 2020;08:174893−174909. [CrossRef]
[26] Dagenet M. Les séchoirs solaires: théorie et pratique. Paris: UNESCO; 1985. p. 575.
[27] Benzaama M-H, Rajaoarisoa L, Boukhelf F, El Mendili Y. Hygrothermal transfer modelling through a bio-based building material: Validation of a switching-linear model. J Build Eng. 2022;55:104691. [CrossRef]
[28] Benzaama M-H, Rajaoarisoa L, Ajib B, Lecoeuche S. A data-driven methodology to predict thermal behavior of residential buildings using piecewise linear models. J Build Eng. 2020;32:101523. [CrossRef]
[29] Arduino (2021). Grove - Temperature and Humidity Sensor Pro